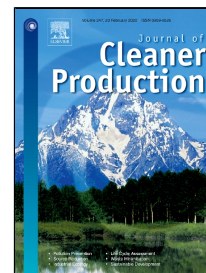


# Journal Pre-proof

The application of the yield approach to study slurry migration in drill cuttings waste underground disposal

Chaobin Guo, Xiaoyu Wang, Cai Li, Keni Zhang, Zuansi Cai



PII: S0959-6526(20)30191-8  
DOI: <https://doi.org/10.1016/j.jclepro.2020.120144>  
Reference: JCLP 120144  
To appear in: *Journal of Cleaner Production*  
Received Date: 16 July 2019  
Accepted Date: 12 January 2020

Please cite this article as: Chaobin Guo, Xiaoyu Wang, Cai Li, Keni Zhang, Zuansi Cai, The application of the yield approach to study slurry migration in drill cuttings waste underground disposal, *Journal of Cleaner Production* (2020), <https://doi.org/10.1016/j.jclepro.2020.120144>

This is a PDF file of an article that has undergone enhancements after acceptance, such as the addition of a cover page and metadata, and formatting for readability, but it is not yet the definitive version of record. This version will undergo additional copyediting, typesetting and review before it is published in its final form, but we are providing this version to give early visibility of the article. Please note that, during the production process, errors may be discovered which could affect the content, and all legal disclaimers that apply to the journal pertain.

© 2019 Published by Elsevier.

## **The application of the yield approach to study slurry migration in drill cuttings waste underground disposal**

Chaobin Guo<sup>1</sup>, Xiaoyu Wang<sup>2</sup>, Cai Li<sup>3</sup>, Keni Zhang<sup>4,\*</sup>, Zuansi Cai<sup>5</sup>

1 Chinese Academy of Geological Sciences, Beijing 100037, China

2 College of Water Sciences, Beijing Normal University, Beijing 100875, China

3 School of Civil Engineering, the University of Sydney, NSW 2006, Australia

4 Institute of Groundwater and Earth Sciences, Jinan University, Guangzhou 510632, China

5 School of Engineering and the Built Environment, Edinburgh Napier University, UK

### **Highlights**

- A numerical model was developed with yield approach for waste underground storage.
- The model has been tested against analytical solutions and a field application.
- A short intermittent injection can lead to an earlier formation breakdown and reduce storage capacity.

### **Abstract**

The underground disposal of drill cuttings waste is a common practice for the gas/oil industry to achieve zero-discharge sustainable development. In this study, a numerical modeling approach was developed to simulate the slurry flow for underground disposal of drill cuttings waste. The modeling approach was coupled with and implemented in the well-known general purpose subsurface multiphase flow simulator, TOUGH2. The new modeling approach treats the slurry flow behavior in subsurface systems as Bingham plastic liquid, with a linear relationship representing the yield stress and the concentration of the gelatinizer in the slurry. In addition, the precipitation-dissolution process was taken into account for solid-aqueous

---

\* Corresponding author: Keni Zhang, Email: [cugbgcb@163.com](mailto:cugbgcb@163.com)

phase changes of the water-slurry mixture under and over the threshold pressure. The model has been verified by the analytical solution of a transient flow of single-phase Bingham fluid, and has further been tested by modeling field-scale injection of drill cutting wastes into a multi-layered geological formation in Texas. A hypothetical model has also been used to conduct sensitivity analysis of the impact of slurry density, injection depth and injection pattern on the storage formation performance. The results revealed that the effect of injection volume is greater than the mass on pressure buildup. In addition, a short period of intermittent reinjection can lead to an earlier formation breakdown due to particle sedimentation and reduce the storage capacity. The developed model can be used to evaluate the prediction of slurry transport, storage capacity, pressure distribution, and the formation breakdown time in a drill cuttings waste disposal project.

**Keywords:** Drill cuttings waste; Yield approaches; Slurry migration; Numerical simulation

### Nomenclature

| Item           | Description                           | Unit                             |
|----------------|---------------------------------------|----------------------------------|
| $c_{xg}$       | concentration of xanthan gum          | kg/bbl                           |
| $dv/dy$        | shear rate                            | -                                |
| $F$            | mass flux                             | kg/(s·m <sup>2</sup> )           |
| $g$            | the vector of acceleration of gravity | m/s <sup>2</sup>                 |
| $G$            | minimum potential gradient            | -                                |
| $h$            | formation thickness                   | m                                |
| $k$            | permeability                          | 10 <sup>-12</sup> m <sup>2</sup> |
| $k_0$          | original permeability                 | 10 <sup>-12</sup> m <sup>2</sup> |
| $k_r$          | relative permeability                 | -                                |
| $M$            | mass per volume                       | kg/m <sup>3</sup>                |
| $n$            | inward normal vector                  | -                                |
| $P$            | pressure                              | Pa                               |
| $P_e$          | effective pressure                    | Pa                               |
| $P_i$          | initial pressure                      | Pa                               |
| $q$            | sinks or sources                      | -                                |
| $r$            | radius                                | m                                |
| $r_{wl}$       | wellbore radius                       | m                                |
| $s$            | saturation                            | -                                |
| $s_s$          | solid saturation                      | -                                |
| $s_{sly(aq.)}$ | slurry saturation in aqueous phase    | -                                |

|                              |  |                          |
|------------------------------|--|--------------------------|
| $s_{s(\text{sly.})}$         | particle saturation in slurry  | -                        |
| $t$                          | time   | s                        |
| $v_1, v_2, v_3$              | fitting coefficients for mixture viscosity                             | -                        |
| $V_n$                        | volume of subdomain $n$  | $\text{m}^3$             |
| $X$                          | mass fraction  | -                        |
| $X_{\beta}^{\kappa}$         | mass fraction of component $\kappa$ in phase $\beta$                   | -                        |
| $X_{\text{sly}(\text{aq.})}$ | slurry mass fraction in aqueous phase                                  | -                        |
| $X_{s(\text{sly.})}$         | particle mass fraction in slurry                                       | -                        |
| $\Gamma$                     | fractional length of the pore bodies                                   | m                        |
| $\Gamma_n$                   | boundary of subdomain $n$  | -                        |
| $\delta(t)$                  | pressure penetration distance  | m                        |
| $\gamma$                     | precipitation coefficient  | -                        |
| $\eta$                       | apparent viscosity   | $\text{Pa}\cdot\text{s}$ |
| $\mu$                        | viscosity  | $\text{m}^2/\text{s}$    |
| $\mu_b$                      | Bingham plastic viscosity coefficient                                  | -                        |
| $\mu_{\text{mix}}$           | mixture viscosity  | $\text{m}^2/\text{s}$    |
| $\mu_w$                      | water viscosity  | $\text{m}^2/\text{s}$    |
| $v$                          | Darcy velocity;  | m/s                      |
| $\rho$                       | density  | $\text{kg}/\text{m}^3$   |
| $\rho_s$                     | density of particles in slurry   | $\text{kg}/\text{m}^3$   |
| $\rho_{\text{sly}}$          | slurry density   | $\text{kg}/\text{m}^3$   |
| $\rho_w$                     | water density  | $\text{kg}/\text{m}^3$   |
| $\rho_{\text{wl}}$           | fluid density in the well  | $\text{kg}/\text{m}^3$   |
| $\tau$                       | shear stress   | Pa                       |
| $\tau_0$                     | yield point  | Pa                       |
| $\phi$                       | porosity   | -                        |
| $\phi_r$                     | fraction of original porosity at which permeability is reduced to zero | -                        |

## Superscripts &amp; Subscripts

|          |                           |
|----------|---------------------------|
| aq       | aqueous phase             |
| $\beta$  | phase (aqueous, solid)    |
| e        | equivalent parameter      |
| i        | initial parameter         |
| $\kappa$ | component (water, slurry) |
| mix      | mixture                   |
| n        | subdomain                 |
| r        | relative parameter        |
| s        | solid                     |
| sly      | slurry                    |
| w        | water                     |
| wl       | wellbore                  |

## 1. Introduction

Large amounts of drill cuttings waste (DCW) are generated by the gas/oil industry each year. How to dispose of this large amount of waste with limited negative environmental impact remains a big challenge to the industry (Bagatin et al., 2014; Shadizadeh et al., 2011). A range of practical methods like landfilling, thermal treatment and stabilization / solidification (S/S) (Kogbara et al., 2017, 2016) as well as underground storage (e.g., Zha et al., 2018) have been employed to dispose of waste over the years. Among these disposal methods, underground injection is a cost-effective and environmentally friendly solution for non-hazardous waste, especially for the drilling wastes from oil-gas wells (de Almeida et al., 2017).

Underground injection of DCW technology started in the late 1980s with small volumes of drill cuttings slurry using either tubular or annular injections (Abou-Sayed et al., 1989). Prior to the injection, the solid waste is ground into suitable sizes (if necessary) and blended with a fluid (often seawater, collected stormwater, other fresh water, used drilling mud, or produced water) to form a viscous slurry (Veil & Dusseault, 2003). The slurry is then injected into underground by pumping, typically through dedicated disposal well or existing wellbores from depleted gas/oil fields. Over the years, slurry underground injection (SUI) technology has been recognized as a reliable waste management option for eliminating environmental liabilities and reducing surface contamination risks among traditional disposal techniques.

There are typically two types of injection methods for SUI technology, namely sub-fracture injection and slurry injection. The sub-fracture injection method involves slurry injection into underground formations at pressures lower than the formation's fracture pressure, while the slurry injection method applies pressure exceeding the fracture pressure. As the sub-fracture injection method does not involve fracturing underground formations, it has often been used to dispose of the DCW in some environmental safety areas. However, the slurry injection method has been widely employed for SUI technology in field applications. Due to the slurry

injection method involving hydraulic fracturing of underground formations, numerical models are often used for site assessments in terms of potential environmental risk of the fracture propagation and the underground waste storage capacity. A numerical study suggests that solid particles' concentration is one of the key parameters used to control the fracture growth direction due to the change of gravity and slurry viscosity (Yamamoto et al., 2004). In addition, potential blockage in both the well and formation by settling of cuttings is one of the major risks in SUI technology (Veil & Dusseault, 2003). Solid particle size in the slurry has been revealed to be a key factor influencing underground storage capacity.

The process of slurry flow plays an important role in the slurry storage assessment. Shioya et al. (2002) used a solid transport model to depict slurry flow with two phases of flow. Yamamoto et al. (2004) further developed the solid transport model by improving the slip velocity formula, while accounting for the effect of solid particles on fluid viscosity. Given the fact that most slurries are non-Newtonian fluid, mainly plastic fluid and pseudoplastic fluid, with various rheological characteristics, it is difficult to represent diverse slurries in different injection environments by one general rheological model. It is even more challenging to incorporate the complex rheology of various slurries, the interaction between the slurry and the fluid flow in subsurface formations, into numerical simulations.

However, the aforementioned solid transport models ignore the miscibility of the slurry with groundwater. Shadizadeh et al. (2011) used the power law relationship to characterize the rheology of slurry, but did not take the particle settlement into consideration. In general, the Bingham fluid model and power law fluid model are the two most common rheological models to represent the drilling fluid. The Bingham model is more suitable for describing plastic fluid, such as slurry with high clay content, like water-based drilling fluid. This type of slurry remains in a state of flocculation at low stresses, while flowing as a viscous fluid at high stress with a linear relationship between shear stress and shear rate at high stresses. The power law model

is suitable for pseudoplastic fluid, such as macromolecular compound slurries and emulsion flows. Pseudoplastic fluid is driven to flow under tiny stresses, and its viscosity decreases under shear strain. The power law model generally underestimates the flow pressure drop for annular injection, while the Bingham model tends to overrate it (Mukherjee et al., 2017). Besides, the Herschel-Bulkley model, Robertson-Stiff model, and Casson model have also been used to characterize fluid rheology. Although these models may more accurately describe the slurry, they are not capable of modeling other rheological properties of slurry, including two-phase flow of a water-slurry mixture and the precipitation-dissolution process. Neither existing analytical solutions nor existing commercial software are capable of performing the parameter sensitivity analysis and safety evaluation (Hongmei et al., 2008).

In this paper, a numerical simulation approach was developed to represent the Bingham-like slurry flow in subsurface systems, using an effective potential gradient to characterize its flow behavior (Wu, 1998). The approach developed in this paper was implemented as a module of TOUGH2 (Zhang et al., 2008; Pruess et al., 1999) and discretized the equations of continua with the integral finite difference method (Narasimhan & Witherspoon, 1976). An analytical solution was developed for numerical model verification, as well as the application of the numerical model to simulate a field-scale test. In addition, a hypothetical model was constructed to evaluate the sensitivity of engineering parameters like the slurry density, injection depth and injection patterns on slurry transport behaviors, storage capacity and the formation breakdown time.

## **2. Theory and Methodology**

### **2.1 Physical Processes and Assumptions**

SUI technology involves grinding DCW into small particles and blending these particles with a fluid (such as seawater, fresh water, drilling mud, or produced water) to form a slurry. The fluid-based slurry, which is reasonable to be considered as a Bingham fluid, mainly

consists of the blending of mudstone and sandstone drill cuttings, bentonite, fresh water and xanthan gum. Injection of this Bingham-like slurry into underground formations is a two-phase flow phenomenon, with water and slurry as the aqueous phase and DCW particles as solid phase. Once the slurry is first injected into a subsurface system, it will be miscible with groundwater. As the slurry injection continues, with the mass fraction of slurry in aqueous phase increasing, the aqueous phase gradually turns into a Bingham fluid. The Bingham fluid stops flowing when the fluid pressure gradient is lower than the threshold. After a time period, the precipitating process can be initiated. The initiation of the particle sediment can change the physical properties (e.g., porosity and permeability) of subsurface formations. Once the pressure gradient increases beyond a threshold value, the sediment will be stirred up again into the slurry, which also leads to a change of the porosity and permeability of subsurface formations. Under this flow condition, the solid particle transport is not taken into consideration. Therefore, the model does not account for slip velocity between solid and fluid, and the particle settlement is treated as the phase conversion of the slurry. Besides, fracture propagation is not considered in this paper, which means that the excess formation pressure is only modeled as a risk of formation breakdown rather than a force to induce fracture propagation.

### 2.3 Bingham Fluid Rheology

Bingham fluid performs with rigidity at low stresses, while with viscoplasticity at high stresses. Eq. (1) generally describes mud flow or slurry in drilling engineering. The shear rate of Bingham fluid increases linearly with shear stress, if the stress is higher than the yield stress.

$$\tau = \eta \frac{dv}{dy} + \tau_0 \quad (1)$$

An effective potential gradient method is employed to characterize Bingham fluid, because it is numerically more efficient than describing the apparent viscosity (Wu, 1998). Bingham fluid flow follows Darcy's law, presented as Eq. (2) and Eq. (3) with an effective potential gradient (Wu, 1998).

$$v = -\frac{kk_r}{\mu_b} \nabla P_e \quad (2)$$

$$P_e = \begin{cases} \text{sgn}(P)(|P| - G) & |P| \geq G \\ 0 & |P| < G \end{cases} \quad (3)$$

The minimum potential gradient  $G$  is controlled by the yield point of Bingham fluid, presented as Eq. (4) (Pascal, 1986), in which  $\alpha$  ( $2.367 \times 10^{-4}$  selected in this work) is an experimental coefficient or a fitting parameter.

$$G = \frac{\alpha \tau_0}{\sqrt{kk_r}} \quad (4)$$

The yield point is mainly under the influence of additives and the medium density. The most commonly used additives for drilling slurry include xanthan gum, ammonium polyacrylate, denatured starch, and cellulose derivative, which increase the viscosity and the carrying capacity of slurry. In the laboratory experiment investigation for this study, the slurry here mainly consists of the blending of mudstone and sandstone drill cuttings, bentonite, fresh water and xanthan gum. Our previous laboratory data show that the relationship between yield point and the concentration of xanthan gum (Fig. 1) can be approximated by a linear model:  $\tau_0 = 27.839 \cdot c_{xg} + 2.338$ , in which  $c_{xg}$  is the concentration of xanthan gum.

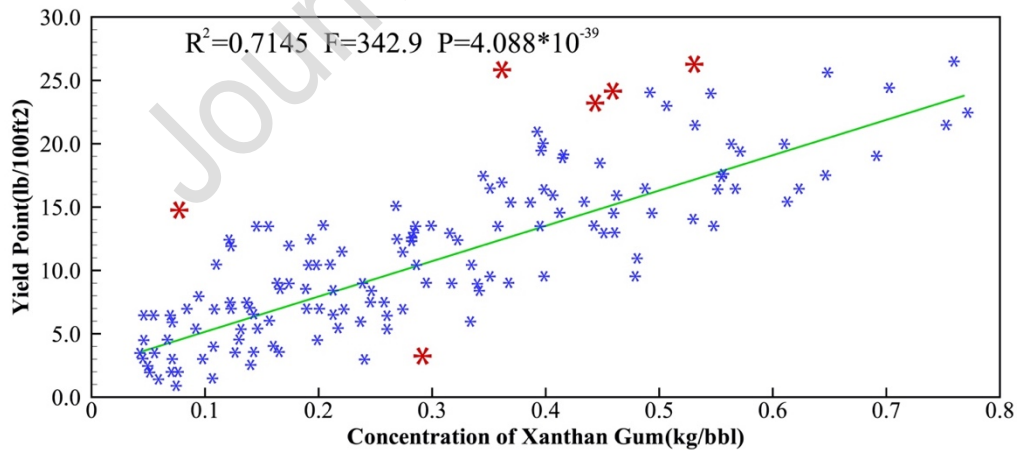


Fig. 1 Yield point versus the concentration of xanthan gum/(kg·bbl-1)

### 3. The implementation of yield approach in TOUGH2

#### 3.1 Numerical solution technique and governing equation

The numerical approach developed for slurry injection was implemented as a module of TOUGH2 (Pruess et al., 1999). The numerical discretization used in the module is the same as TOUGH2. Space is discretized by the integral finite difference method, in the integral form of the conservation equations (Eq. (1)), which is applicable to regular or irregular discretization in one, two, and three dimensions. Time is discretized fully implicitly as a first-order backward finite difference to provide stability.

The nonlinear equations are solved simultaneously by using the Newton-Raphson iteration procedure. On the basis of the convergence criteria of the iteration process, time step is self-adjusting during simulation to speed up simulation times and cut down space storage requirements. The robustness and efficiency of the numerical solution technique have been tested by TOUGH2, in many simulations from theoretical studies to field applications.

The subsurface fluid flow system contains two components – water and slurry, and two phases – aqueous and solid. Water always remains in the aqueous phase, while slurry converts between the solid phase and aqueous phase via the precipitation–dissolution process. The solid phase is immobile. Fluid advection of each component follows the multiphase Darcy’s law. The mass balance equation is described as Eq. (5). Eq. (6) gives the evaluation of mass accumulation term. Fluid flux calculation follows Eqs. (7) and (8).

$$\frac{d}{dt} \int_{V_n} M^\kappa dV_n = \int_{\Gamma_n} F^\kappa \cdot \mathbf{n} d\Gamma_n + \int_{V_n} q^\kappa dV_n \quad (5)$$

$$M^\kappa = \phi \sum_{\beta} S_{\beta} \rho_{\beta} X_{\beta}^{\kappa} \quad (6)$$

$$F^\kappa = \sum_{\beta} F_{\beta} X_{\beta}^{\kappa}. \quad (7)$$

$$F_{\beta} = -k \frac{k_{r\beta} \rho_{\beta}}{\mu_{\beta}} (\nabla P_{\beta} - \rho_{\beta} \mathbf{g}) \quad (8)$$

### 3.2 Mixture Fluid Properties

The pore space in the subsurface formation is occupied by aqueous and solid phases. The aqueous phase consists of water and slurry while the solid phase consists of the sediment of slurry. The salinity of the aqueous phase is characterized by the mass fraction of slurry. The

aqueous phase is assumed to be an ideal fluid with additivity, for which the expansivity and compressibility of water and slurry are treated to be equal at all temperatures and pressures. In this case, it is reasonable to depict the density of water-slurry mixture by Eq. (9) and Eq. (10):

$$\frac{1}{\rho_{mix}} = \frac{X_{sly}}{\rho_{sly}} + \frac{1 - X_{sly}}{\rho_w} \quad (9)$$

$$\frac{\rho_{sly}(P,T)}{\rho_{sly}(P_0,T_0)} = \frac{\rho_w(P,T)}{\rho_w(P_0,T_0)} \quad (10)$$

where  $\rho_w(P_0, T_0)$  and  $\rho_{sly}(P_0, T_0)$  are the density of water and slurry, respectively, at the reference pressure ( $P_0$ ) and temperature ( $T_0$ ).

The viscosity of the water-slurry mixture is estimated by salinity effect with a polynomial correction to the water viscosity shown as Eq. (11) and Eq. (12) (Herbert et al., 1988):

$$\mu_{mix}(P,T,X_{sly}) = \mu_w(P,T)f(X_{sly(aq.)}) \quad (11)$$

$$f(X_{sly(aq.)}) = 1 + v_1X_{sly(aq.)} + v_2X_{sly(aq.)}^2 + v_3X_{sly(aq.)}^3 \quad (12)$$

### 3.3 Precipitation-Dissolution Model

At low shear stresses (lower than the threshold  $G$ ), the Bingham mixture remains in a state of flocculation, and gradually precipitates after a short period of time. At high shear stresses, the sediment will be stirred up again into the slurry, and flows as a viscous fluid. This precipitation-dissolution process was considered to be the phase conversion of the slurry. In this study, a set of mass conservation equations was used to represent the phase conversion of the Bingham mixture, where the ratio of the slurry density and aqueous mass fraction of slurry are expressed as a function of the density of water and solid as well as solid saturation (Eq. (13)). The solid phase here includes both drill cuttings and additives.

$$M_{mix} = M_s + M_w \Rightarrow \frac{\rho_{sly}}{X_{sly(aq.)}} = \rho_s S_s + \rho_w (1 - S_s) \quad (13)$$

In addition, solid particle sediment is considered as the main cause of the mass change of the Bingham mixture. Therefore, the mass change rate of the mixture is represented as a function of a first-order precipitation rate of the particles, the slurry aqueous mass fraction and

the density of the Bingham mixture (Eq. (14)), by ignoring the impact of temperature and particle size.

$$\frac{dM_{mix}}{dt} = -\gamma X_{sly(aq.)} \rho_{mix} \quad (14)$$

The solid particle sediment can reduce the porosity and permeability of the host geological formation. Therefore, the change of porosity here is represented by solid saturation. However, the impact of solid particle sediment on permeability is rather complex. This is not only because it reduces the porosity which can lead to the reduction of permeability, but also because it changes the shape of the pore body. For example, the clog in pore throats due to the solid particle sediment could result in a big reduction in permeability. The permeability change is, therefore, represented by the tubes-in-series model which contains tubes with different radii in series (Fig. 2 and Eq. (15)) and permeability was reduced to zero at a finite porosity (Verma & Pruess, 1988). A parallel-plate model with Eq. (18) can be implemented to describe the fracture segments of different apertures in series and a straight tubes model with Eq. (19) can be used for only straight capillary tubes of uniform radius (Verma & Pruess, 1988). The relative change in permeability  $k/k_0$  is:

$$\frac{k}{k_0} = \theta^2 \frac{1 - \Gamma + \Gamma/\omega^2}{1 - \Gamma + \Gamma[\theta/(\theta + \omega - 1)]^2} \quad (15)$$

$$\theta = \frac{1 - s_s - \phi_f}{1 - \phi_f} \quad (16)$$

$$\omega = 1 + \frac{1/\Gamma}{1/\phi_f - 1} \quad (17)$$

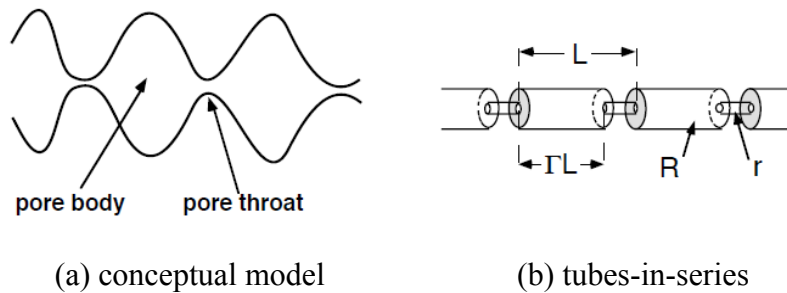


Fig. 2 Model for converging-diverging pore channels

$$\frac{k}{k_0} = \theta^3 \frac{1 - \Gamma + \frac{\Gamma}{\omega^3}}{1 - \Gamma + \Gamma[\theta/(\theta + \omega - 1)]^3} \quad (18)$$

$$\frac{k}{k_0} = (1 - s_s)^2 \quad (19)$$

## 4. Result and Discussion

### 4.1 Comparison with analytical solution

A transient flow model of single-phase Bingham fluid, without accounting for precipitation, was developed in this study for the numerical model verification (Eq. (20)). The model considers the injection of a single phase of Bingham liquid with a constant pumping rate, in an infinite homogeneous and horizontal reservoir with a constant thickness of a sandstone formation. The detailed parameter values for the model are listed in Table 1.

$$P(r,t) = P_i + [r - (r_w + \delta(t))]G - \frac{q(t)\mu_b}{2\pi kh\rho_w(P)} \left[ \frac{1 + \frac{2\delta(t)}{r_w}}{\frac{2\delta(t)}{r_w}} \right] \ln \left[ \frac{2r}{r_w + \delta(t)} - \left( \frac{r}{r_w + \delta(t)} \right)^2 \right] \quad (20)$$

In the analytical solution, the wellbore fluid density  $\rho_w$  and pressure penetration distance  $\delta(t)$  are valued by the numerical result. The results of comparing the pressure variation show a good match between the numerical model and the analytical solution (Fig. 3 & 4), indicating the reliability of the numerical method.

Table 1 Parameters for transient flow of single-phase Bingham fluid

| Parameter           | Value              | Parameter                            | Value                       |
|---------------------|--------------------|--------------------------------------|-----------------------------|
| Porosity            | 0.2                | Initial density                      | 1226 kg/m <sup>3</sup>      |
| Permeability        | 1 Darcy            | Plastic viscosity                    | 0.021 Pa·s                  |
| Wellbore radius     | 0.1 m              | Yield point                          | 14.09 lb/100ft <sup>2</sup> |
| Initial pressure    | 10 <sup>7</sup> Pa | Minimum potential gradient $G$       | 1600 Pa/m                   |
| Formation thickness | 1 m                | Coefficient $\alpha$ for $G$ in Eq.8 | 2.367×10 <sup>-4</sup>      |
| Pumping rate        | 1 kg/s             | Concentration of xanthan gum         | 0.422 kg/bbl                |

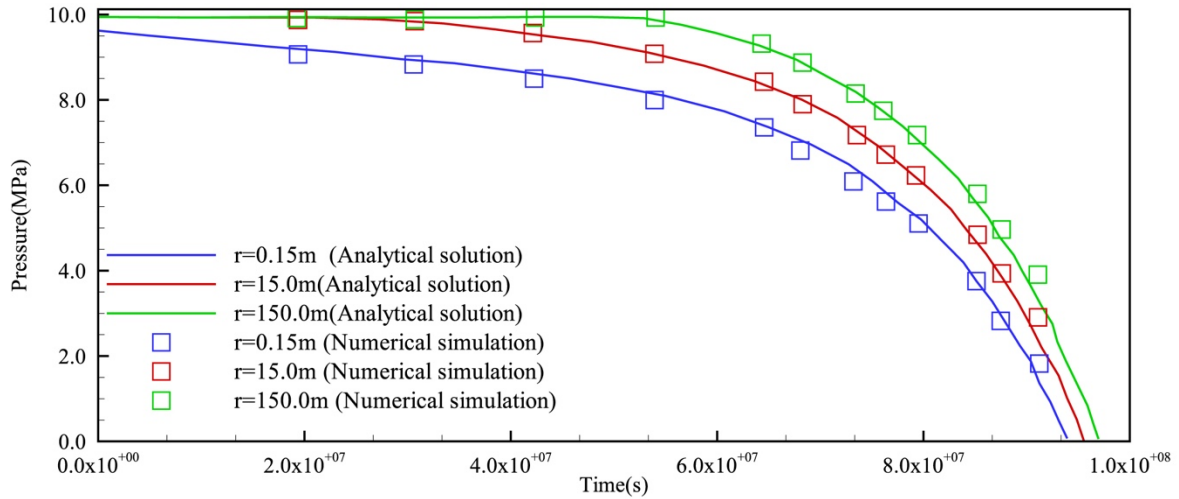


Fig. 3 Comparison of the pressure profiles at  $r=0.15$  m, 15 m, and 150 m for numerical and analytical solutions

The analytical verification also suggested that the numerical method could introduce uncertainty as a result of the linear yield point model. According to the regression analysis of our experiment (Fig. 1), the linear relationship between yield point and the concentration of additive (xanthan gum) was not well performed with the goodness of fit  $R^2=71.45\%$ . Besides, it could be problematic to determine to what extent the mixture should be treated as Bingham fluid. Numerical experiments show that the choice of different criteria, based on the mass fraction of slurry in the aqueous phase, makes a small difference in numerical performance. In this study, the water-slurry mixture was treated as Bingham fluid, with the mass fraction of slurry greater than 0.8.

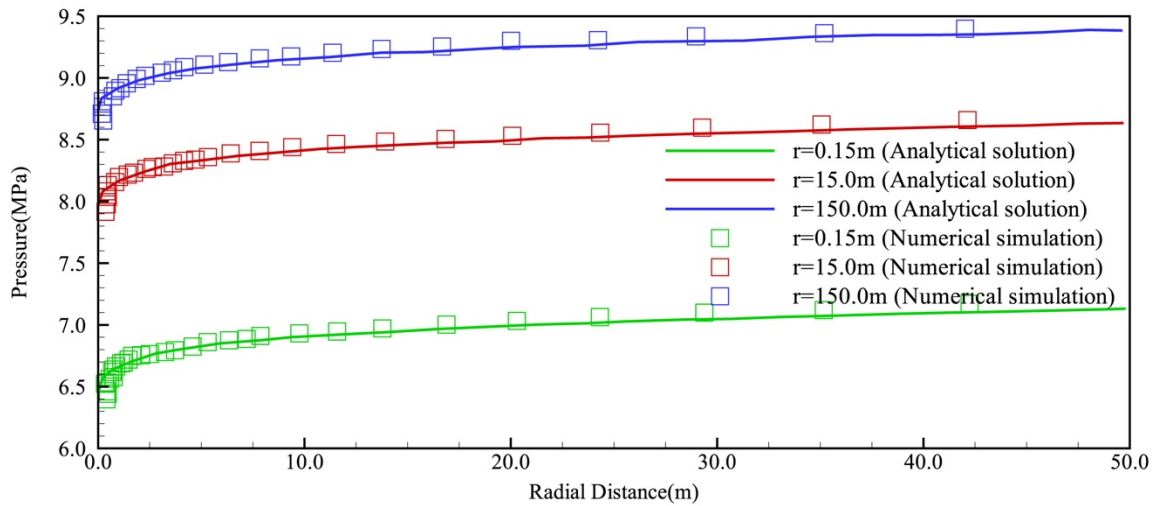


Fig. 4 Comparison of the pressure at  $t=1d, 10d, 100d$  for numerical and analytical solutions along the radial distance

#### 4.2 Field test comparison

A pilot SUI project has been conducted in Live Oak, Texas to dispose of DCW into the geological formations at a depth of 2,000 m below ground surface (bgs). The project aimed to inject DCW into three sandstone formations, with a total thickness of 144.8 m. These three sandstone layers have decreasing permeability and porosity with depth (selected hydrogeological properties in Table 2). The top formation at a depth from 2,122.9 m to 2,139.7 m bgs has a relatively high permeability and a porosity of 24%. This formation is suitable for slurry injection. The middle formation at a depth from 2,162.9 m to 2,201.3 m bgs has fair permeability and a porosity of 20%. In this formation, the suitable injection scheme should be decided according to injection tests. The bottom formation at a depth from 2,262.2 m to 2,267.7 m bgs is less permeable and its porosity is only 15%. This formation may only be suitable for water injection. These three formations are continuously distributed. A vertical well was drilled to penetrate through these three formations. Due to the leakage risk considerations, only middle and bottom formations were perforated for injection, and the top formation was used as a buffer zone. Slurrified DCW was intermittently injected into the middle formation at a depth of 2,174 m bgs.

A site-scale model was constructed in this study according to the field measured data. The model domain covers an area of  $9 \text{ km} \times 9 \text{ km}$  with a thickness of 300 m with a depth from 2,000 m to 2,300 m bgs (Fig. 5). The injection well is located at the center of the model domain. The grids at the locations of wellbore, interface between overlying boundary and target aquifer have been refined. The sandstone formations were discretized into seven model layers (Lyr01 ~ Lyr07), which are interlayered by mudstone formations. Only Lyr04 ~ Lyr07 are perforated as an injection zone.

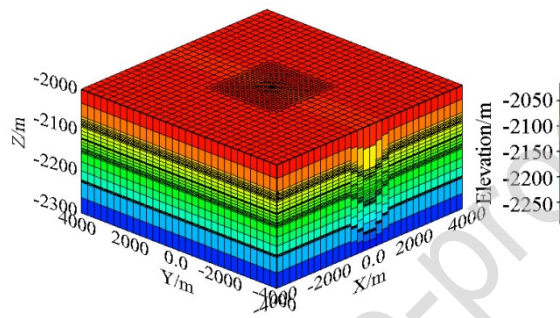


Fig. 5 Model for Texas SUI project

Table 2 Hydrogeologic parameters

| Model layer | Lithology | Permeability/mD | Porosity |
|-------------|-----------|-----------------|----------|
| Lyr01~03    | sandstone | 243             | 0.24     |
| Lyr04~06    | sandstone | 95              | 0.20     |
| Lyr07       | sandstone | 40              | 0.15     |
| aquiclude   | mudstone  | 0.01            | 0.15     |

As the permeability data of the formations has not been measured. The permeability of each sandstone layer was estimated based on an empirical value related to the porosity (shown in Ehrenberg & Nadeau, 2005). Hydrostatic pressure was set as initial conditions. The first-type boundary was applied to four-side boundaries. Top and bottom were assumed to be impermeable. In this study, the first 50 days of intermittent injection operation (Table 3) were simulated. The injection materials consist of slurrified DCW, water and gelatinizer (xanthan

gum). In the simulation, the xanthan gum, treated as part of the slurry component, was supplemented by water in order to match the reference slurry density of  $1,250 \text{ kg}\cdot\text{m}^{-3}$ .

Table 3 Texas oilfield SUI injection scheme

| Date           | Injection | Shut-in | Xanthan | Slurry/bbl | Water/bbl |
|----------------|-----------|---------|---------|------------|-----------|
| year/month/day | Time/s    | Time/s  | Gum/bbl |            |           |
| 2014/3/30      | 6:10      | 9:33    | 36      | 804        | 250       |
| 2014/3/31      | 16:10     | 18:10   | 0       | 0          | 0         |
| 2014/4/1       | 16:00     | 17:10   | 19      | 50         | 0         |
| 2014/4/2       | 0:10      | 6:28    | 42      | 1646       | 367       |
| 2014/4/3       | 8:00      | 12:05   | 39      | 989        | 280       |
| .....          | .....     | .....   | .....   | .....      | .....     |
| 2014/5/14      | 15:15     | 20:59   | 25      | 1329       | 732       |
| 2014/5/15      | 20:14     | 23:59   | 25      | 1672       | 230       |
| 2014/5/16      | 09:38     | 19:37   | 28      | 2143       | 270       |
| 2014/5/17      | 02:33     | 20:53   | 22      | 1004       | 0         |
| 2014/5/18      | 02:12     | 23:53   | 50      | 1714       | 932       |

The results show that the modeled pressure profile, in general, matches the monitoring data well (Fig. 6). There are some big deviations between the numerical result and monitoring data at around Day 25. This might be as a result of the fracture propagation at this stage of the field operation as the numerical approach developed in this study is not capable of modeling the mechanical processes of fracture propagation. Anyway, the model reproduces the pressure profile at the early stage of slurry injection well.

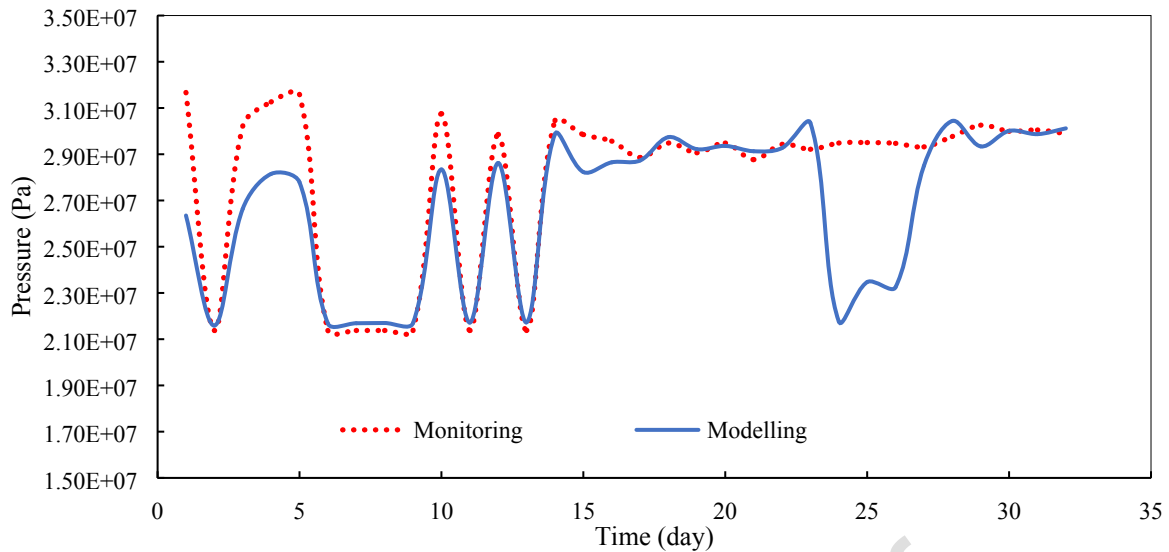


Fig. 6 Pressure comparison of the monitoring and modeling result

The pressure, slurry, and solid precipitation distribution at day 30 were chosen to investigate the performance of numerical simulation of the Texas SUI project. The pressure spreads away in Lyr4 and the layers below, within a radius of about 4,000 m. The slurry migrates about 30 m away from the injection well after day 30, and the pressure gradient at this point is high enough to ensure that solid particles remain in suspension for further migration along the injection layer, Lyr4. Once the slurry spreads further, the pressure gradient decreases and solid particles begins to precipitate. Thus, the solid precipitation mostly accumulates at the front of the slurry plume which is about 200 m away from the wellbore.

#### 4.3 Impact assessment of geological parameters

A hypothetical model was constructed to evaluate the sensitivity of engineering parameters, where the model contains three sandstone formations and two mudstone aquicludes. A radial model was established with the domain of  $R = 10$  km, which was to ensure the boundary as the first-type boundary, with a thickness of 60 m from the depth at  $\sim 1,900$  m bgs to  $\sim 1,960$  m bgs. The model domain was discretized with a grid width from 2 m to 50 m, and vertically 22 model layers (Fig. 7). The middle sandstone formation with four model layers was perforated for reinjection. Hydrostatic pressure was used as the initial conditions. All

model parameter values are listed in Table 4. The reference slurry had the density of 1,250 kg/m<sup>3</sup> and viscosity of 21 mPa·s which contains the gelatinizer (xanthan gum) of 0.422 kg/bbl. The slurry precipitation process was assumed to start in an hour once the pressure gradient was less than or equivalent to the threshold gradient  $G$ , while the dissolution begins when the pressure gradient is greater than 2.5 times  $G$ . The change of formation permeability due to the precipitation-dissolution process was represented by the straight tubes model. In this study, sensitivity analysis was conducted to investigate the impact of slurry density, injection depth and intermittent injection scheme on underground storage capability.

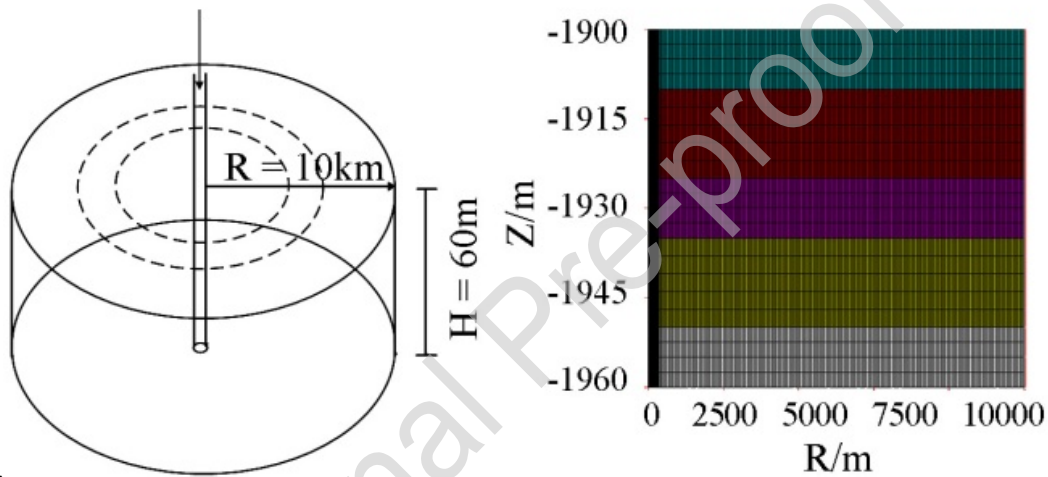


Fig. 7 Radial-symmetric model

Table 4 Hydrogeologic parameters

| Parameter              | Value                            | Remark                        |
|------------------------|----------------------------------|-------------------------------|
| porosity               | 0.24                             |                               |
| sandstone permeability | $2.0 \times 10^{-13} \text{m}^2$ | $k_x = k_y = 10k_z$           |
| mudstone permeability  | $1.0 \times 10^{-17} \text{m}^2$ | $k_x = k_y = 10k_z$           |
| breakdown pressure     | $1.5 \times P_0$                 | $P_0$ is hydrostatic pressure |

#### 4.3.1 The Impact of Slurry Density and Injection Volume

Slurry reinjection with different densities between 1,050 and 1,350 kg/m<sup>3</sup> was conducted to investigate the slurry flow pattern and pressure distribution. The slurry density was defined as the density of the DCW and supplementary water mixture. Three rejection cases were

investigated with the same mass of slurry (case a), the same mass/volume of DCW (b), and the same volume of slurry (c) respectively. In each case, the slurrified DCW was continuously injected until the formation breakdown or for 10 years. The injection rate for each case is listed in Table 5, and other model parameters are the same as those of the reference slurry.

Table 5 Different injection rate cases under unequal slurry density

| Slurry Density /<br>( $\text{kg}\cdot\text{m}^{-3}$ ) | Injection Rate/ ( $\text{kg}\cdot\text{s}^{-1}$ ) |                                     |  |
|---|---|-------------------------------------|--|
|   | a<br>(With the same<br>mass of slurry)            | b<br>(With the same mass of<br>DCW) | c<br>(With the same<br>volume of slurry) |
| 1050  | 2.00  | 8.40                                | 1.68                                     |
| 1100  | 2.00  | 4.40                                | 1.76                                     |
| 1150  | 2.00  | 3.07                                | 1.84                                     |
| 1200  | 2.00  | 2.40                                | 1.92                                     |
| 1250  | 2.00  | 2.00                                | 2.00                                     |
| 1300  | 2.00  | 1.73                                | 2.08                                     |
| 1350  | 2.00  | 1.54                                | 2.16                                     |

The formation was assumed to be fractured when pressure buildup exceeded 9.405 MPa (a half of the hydrostatic pressure). For reinjecting the same mass of slurry (Fig. 8a) or drill cuttings (Fig. 8b), slurry with lower density tends to lead to earlier formation breakdown, while it is quite preferable for fracture propagation. However, it makes little difference in pressure oscillation for slurry reinjection with the same volume (Fig. 8c). Comparing case (a) and (b) with case (c), the injection volume has a more observable impact than slurry density on pressure fluctuation of the formation. Larger injection volume leads to a higher pressure increment, and earlier formation breakdown. In a SUI project, when a certain amount of drill cuttings is about

to be processed (goes as case b shown in Fig. 8b), the injection scheme with a lower slurry density means a larger injection volume of slurry, which would aggravate the difficulty of disposal and probably cause a breakdown risk.

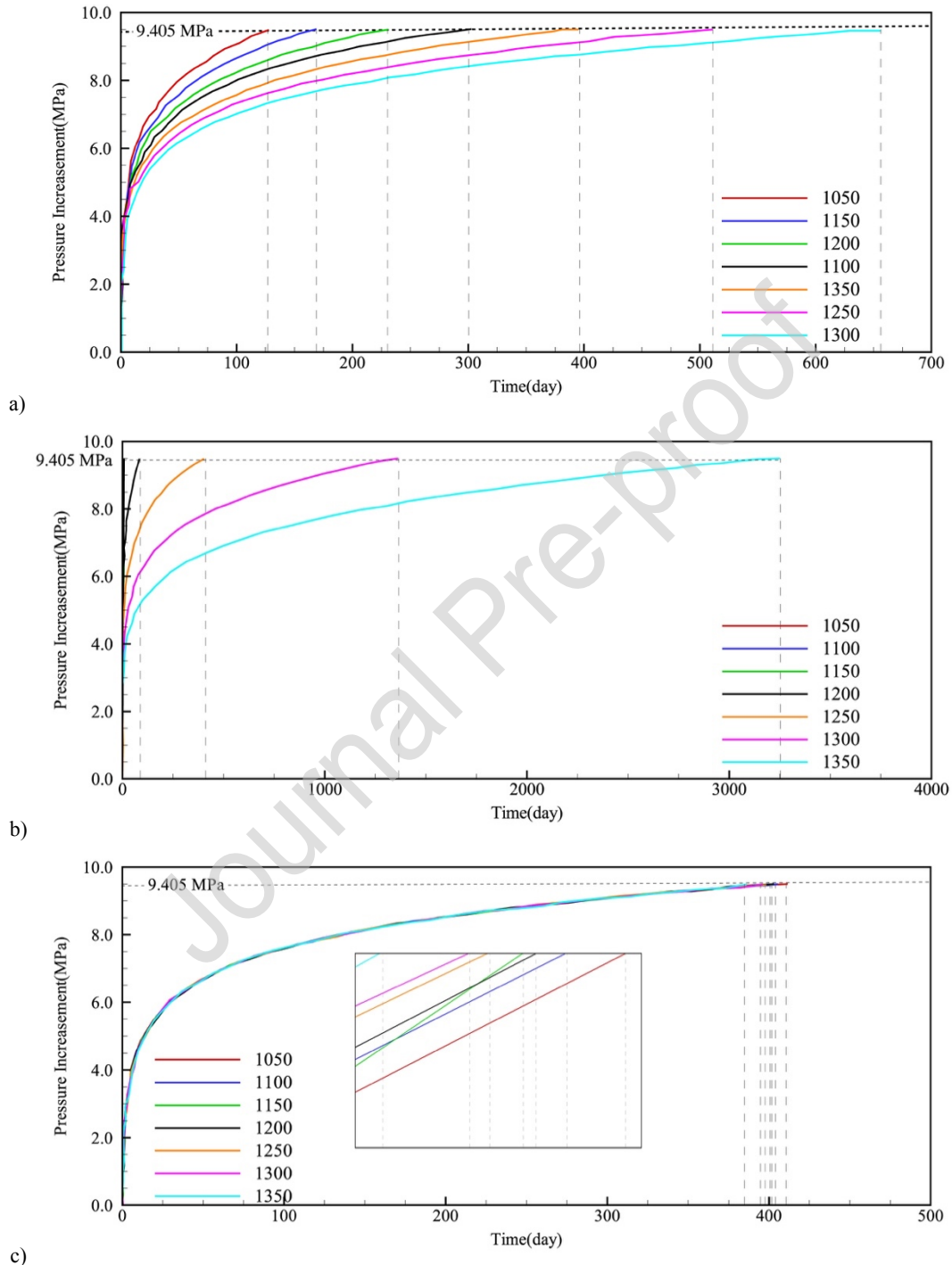


Fig. 8 Simulated maximum pressure increments under different slurry density cases with the same mass of slurry (case a), the same mass/volume of drill cuttings (case b) and the same volume of slurry (case c)

#### 4.3.2 The Impact of Injection Depth

A deeper injection depth means safer disposal and a less economical project, so the suitable injection depth is an important factor for SUI applications. Different injection depth schemes (-925 m to -2,425 m) are designed to conduct the analysis. Other model parameters are the same as that of the basic slurry model.

Model results show that it only takes 2.41 days for the pressure buildup to reach the formation down pressure for the injection depth of 925 m bgs, but more than 10 years at 2,175 m bgs (Fig. 9). This suggests that shallower injection means less pressure buildup for the formation breakdown, which could induce fracture propagation. Induced fracture propagation can be favorable for enhancing injectivity. However, fracture propagation can lead to a potential risk of leakage. Therefore, slurry injection depth should be carefully designed, especially for less permeable formations.

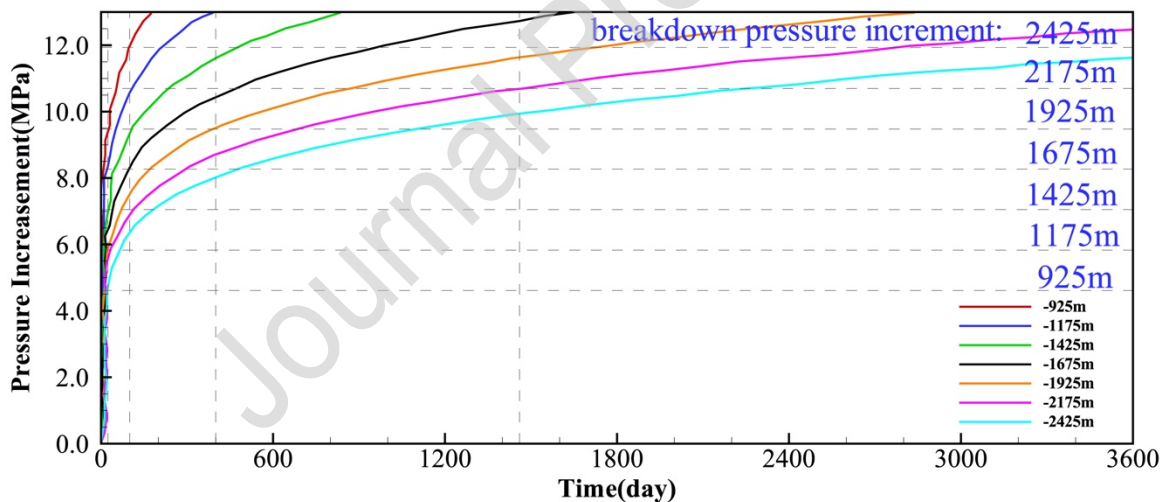


Fig. 9 Simulated maximum pressure increases under different injection depth cases

#### 4.3.3 The Impact of Injection Pattern

The pressure oscillation and slurry precipitation can be significantly impacted by intermittent injection. Intermittent injection cases with different shut-in periods were simulated, and compared with two continuous injection cases. The injection parameters are listed in Table 6. Other model parameters are the same as that of the reference slurry model.

Table 6 Different cases of intermittent injection

|                        | Injection rate/(kg·s <sup>-1</sup> ) | Shut-in period/d |
|------------------------|--------------------------------------|------------------|
| Continuous injection   | 1                                    | -                |
|                        | 2                                    | -                |
| Intermittent injection | 2                                    | 10               |
|                        |                                      | 20               |
|                        |                                      | 40               |
|                        |                                      | 60               |
|                        |                                      | 120              |

The results show that the pressure distribution, the mass of sediment and the amount of slurry injection exhibit periodical change for different intermittent injection cases. The formation pressure quickly increases during the injection time and rapidly decreases at the beginning of shut-in (Fig. 10). The formation tends to reach breakdown pressure much earlier in the intermittent injection cases than the continuous injection cases. This is because most particles settle during the shut-in period, while this is not the case during injection periods (Fig. 11). Short periods of intermittent reinjection lead to an earlier formation breakdown, which may be favorable for fracturing reinjection.

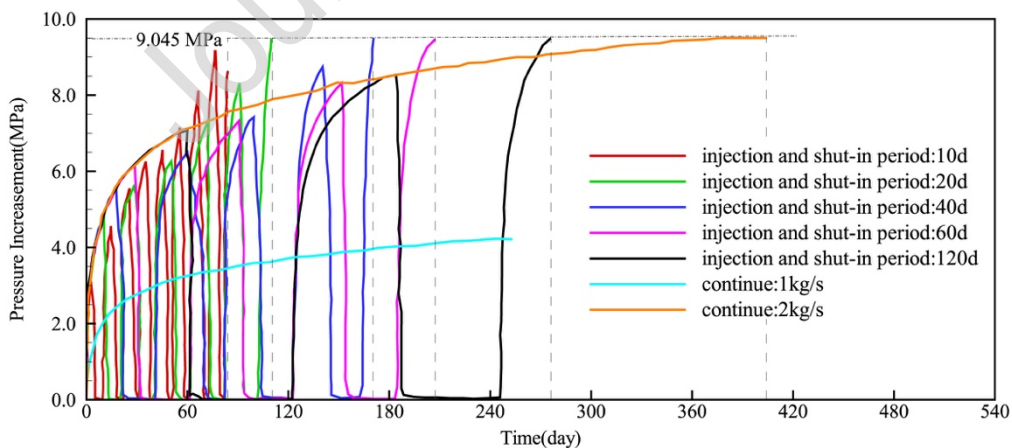


Fig. 10 Simulated maximum pressure increments under different intermittent injection cases

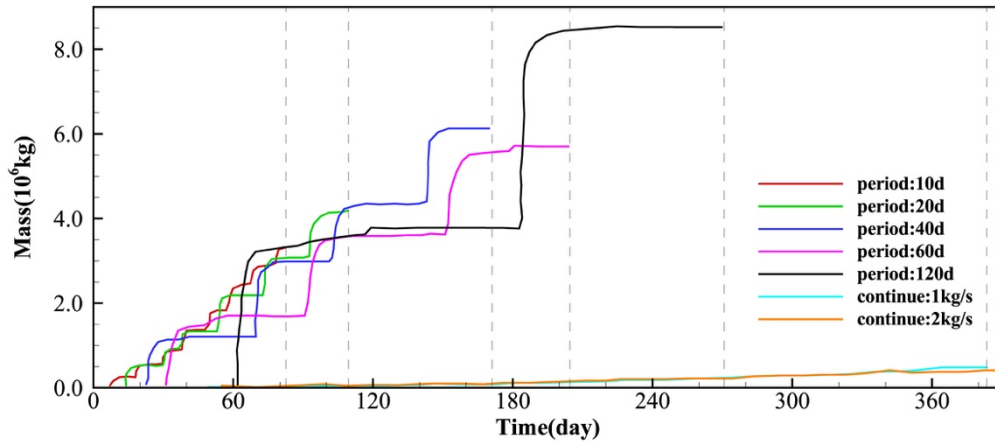


Fig. 11 Simulated mass of the particle sediment under different intermittent injection cases

## 5. Conclusion

Drilling cuttings waste can be disposed of underground through slurry injection. Numerical simulation offers a useful tool to quantify the complex processes of the slurry flow in subsurface geological formations. We have successfully developed a numerical modeling method for the simulation of the slurry injection processes. In this study, the numerical method treated the slurry as a Bingham-like liquid, by incorporating the yield approach for representation of the shear stress to initiate the slurry flow. A linear relationship between the yield point and concentration of the gelatinizer (xanthan gum) in slurry was used based on our previous experimental data. Besides, the precipitation-dissolution process of the Bingham water-slurry mixture, and the impact of this process on formation permeability and porosity were taken into full consideration in the new numerical model.

The numerical model was verified with an analytical solution of a transient flow of single-phase Bingham fluid in a homogeneous geological formation, without the consideration of precipitation of the solid particles. Furthermore, the numerical model was applied to simulate a field application of the SUI injection in Texas. The results confirmed that the model is capable of modeling the complex slurry flow processes including the precipitation-dissolution process in the multi-layered geological settings. Sensitivity analysis was conducted of the impact of the slurry density, injection depth and slurry injection pattern on the storage capability through an

idealized hypothetical case. The model suggested that the injection volume has a more observable impact than slurry density on pressure fluctuation of the formation. In addition, a short period of intermittent reinjection can significantly lead to early formation breakdown.

The developed modeling approach can be used to investigate the slurry transport, storage capacity, pressure distribution, and formation breakdown time for slurry underground injection project planning and performance evaluation. Engineering parameters should be carefully designed to mitigate potential environmental risks of the fracture propagation. Therefore, the future development of the modeling capability shall account for the mechanical response along with the injection process. In addition, influence of porosity and permeability heterogeneity is also required for further study.

### **Acknowledgement**

This work was partially sponsored by the Chinese Academy of Geological Sciences Research Fund (YWF201903, JYYWF20180301, YYWF201735), Geological Survey Project (No. DD20179611, CDD1919), the funding support from the Lawrence Ho Research and development fund and Jereh Energy Services Corporation.

### **References**

- Abou-Sayed, A.S., Andrews, D.E., Buhidma, I.M., 1989. Evaluation of oily waste injection below the permafrost in Prudhoe Bay Field.
- Bagatin, R., Klemeš, J.J., Reverberi, A. Pietro, Huisingh, D., 2014. Conservation and improvements in water resource management: A global challenge. *J. Clean. Prod.* <https://doi.org/10.1016/j.jclepro.2014.04.027>
- de Almeida, P.C., Araújo, O. de Q.F., de Medeiros, J.L., 2017. Managing offshore drill cuttings waste for improved sustainability. *J. Clean. Prod.* <https://doi.org/10.1016/j.jclepro.2017.07.062>
- Ehrenberg, S.N., Nadeau, P.H., 2005. Sandstone versus carbonate petroleum reservoirs: A global perspective on porosity-depth and porosity-permeability relationships, in: 67th

- European Association of Geoscientists and Engineers, EAGE Conference and Exhibition, Incorporating SPE EUROPE2005 - Extended Abstracts.
- Herbert, A.W., Jackson, C.P., Lever, D.A., 1988. Coupled groundwater flow and solute transport with fluid density strongly dependent upon concentration. *Water Resour. Res.* <https://doi.org/10.1029/WR024i010p01781>
- Hongmei, T., Xiaoming, W., Hongliang, N., 2008. The optimization of rheological model. *Trenchless Technol.* 25, 1–4.
- Keni Zhang, Yu-shu Wu, K.P., 2008. User's Guide for TOUGH2-MP- A Massively Parallel Version of the TOUGH2 Code. Lawrence Berkeley Natl. Lab.
- Kogbara, R.B., Ayotamuno, J.M., Onuomah, I., Ehio, V., Damka, T.D., 2016. Stabilisation/solidification and bioaugmentation treatment of petroleum drill cuttings. *Appl. Geochemistry* 71, 1–8. <https://doi.org/10.1016/j.apgeochem.2016.05.010>
- Kogbara, R.B., Dumkhana, B.B., Ayotamuno, J.M., Okparanma, R.N., 2017. Recycling stabilised/solidified drill cuttings for forage production in acidic soils. *Chemosphere* 184, 652–663. <https://doi.org/10.1016/j.chemosphere.2017.06.042>
- Mukherjee, S., Gupta, A.K., Chhabra, R.P., 2017. Laminar forced convection in power-law and Bingham plastic fluids in ducts of semi-circular and other cross-sections. *Int. J. Heat Mass Transf.* 104, 112–141. <https://doi.org/10.1016/j.ijheatmasstransfer.2016.08.007>
- Narasimhan, T.N., Witherspoon, P.A., 1976. An integrated finite difference method for analyzing fluid flow in porous media. *Water Resour. Res.* <https://doi.org/10.1029/WR012i001p00057>
- Pascal, H., 1986. A theoretical analysis on stability of a moving interface in a porous medium for bingham displacing fluids and its application in oil displacement mechanism. *Can. J. Chem. Eng.* <https://doi.org/10.1002/cjce.5450640303>
- Pruess, K., Oldenburg, C., Moridis, G., 1999. TOUGH2 User's Guide Version 2.0, Report LBNL-43134, Lawrence Berkeley National Laboratory, California Lawrence Berkeley National Laboratory.
- Shadizadeh, S.R., Majidaie, S., Zoveidavianpoor, M., 2011. Investigation of drill cuttings reinjection: Environmental management in iranian ahwaz oilfield. *Pet. Sci. Technol.* <https://doi.org/10.1080/10916460903530473>
- Shioya, Y., Yamamoto, K., Fujieda, T., Kikuchi, S., El-Khatib, H., 2002. Cuttings reinjection to shallow undersea formation: The Geomechanical acceptance analysis using hydraulic fracturing simulator, in: Society of Petroleum Engineers - Abu Dhabi International Petroleum Exhibition and Conference 2002, ADIPEC 2002.

- Veil, J.A., Dusseault, M.B., 2003. Evaluation of slurry injection technology for management of drilling wastes. <https://dx.doi.org/10.2172/819455>
- Verma, A., Pruess, K., 1988. Thermohydrological conditions and silica redistribution near high-level nuclear wastes emplaced in saturated geological formations. *J. Geophys. Res.* <https://doi.org/10.1029/JB093iB02p01159>
- Wu, Y., 1998. A numerical method for simulating non-Newtonian fluid flow and displacement in porous media. *Adv. Water Resour.* 21, 351–362.
- Yamamoto, K., Koyama, T., Nakama, Y., 2004. Geometry of the fracture for cuttings reinjection operation and solid concentration: A numerical study, in: *Gulf Rocks 2004 - 6th North America Rock Mechanics Symposium, NARMS 2004*.
- Zha, X., Liao, X., Zhao, X., Liu, F., He, A.Q., Xiong, W.X., 2018. Turning Waste drilling fluids into a new, sustainable soil resources for landscaping. *Ecol. Eng.* <https://doi.org/10.1016/j.ecoleng.2017.06.026>

**Author Contribution Statement**

**Chaobin Guo:** Conceptualization, Methodology, Software, Validation.

**Xiaoyu Wang:** Data curation, Writing- Original draft preparation.

**Cai Li:** Visualization, Investigation.

**Keni Zhang:** Supervision.

**Zuansi Cai:** Writing- Reviewing and Editing.

Journal Pre-proof

**Declaration of interests**

The authors declare that they have no known competing financial interests or personal relationships that could have appeared to influence the work reported in this paper.

The authors declare the following financial interests/personal relationships which may be considered as potential competing interests:

Journal Pre-proof